# CHARACTERISATION OF WELD METAL FOR 3.5% NICKEL STEEL IN MANUAL METAL ARC WELDING AND ITS STRESS CORROSION AND LOW CYCLE CORROSION FATIGUE PROPENSITIES

* P. Kumar. P. Majumdar, T. K. Pal
Department of Metallurgical Engineering
Jadavpur University, Calcutta 700 032

*PG Res. Student

## INTRODUCTION

3.5% nickel steel possesses a combination of high strength and resistance to brittle fracture which makes it suitable to be widely used for the fabrication of storage tanks designed to be used at between 223K and 172K (pressure vessels to produce ethylene or propylene from naptha in chemical plant)[1-4]. These structures are fabricated, typically, by manual metal arc welding with coated electrodes. Though many electrodes are marginally satisfactory at 172K, the weld metal toughness is the limiting criteria for such grade of steel. Globally, failure of 3.5% nickel steel all weld containers are known. During 60's the failure of LPG tankers led to R & D works in USA and Japan [5]. To enhance the safety of these structures, under cryogenic service conditions, adequate fracture properties, particularly low temperature toughness, need to be assessed.

It is now well established that the presence of acicular ferrite in the primary microstructure of low alloy steel weld deposits leads to improved toughness [6, 7].

In this project work, assessment of cryogenic toughness properties of weld metal produced by microstructural development through controlled heat input and thereby inducing the effect of acicular ferrite has been attempted. Subsequently, environment sensitive failure effects were characterised as stress corrosion (SC) and low cycle corrosion fatigue (LCCF) failure.

## EXPERIMENTAL PROCEDURE

### Experimental steel and joint preparation

3.5% nickel steel plates of sizes 450mm x 160mm x 12mm were procured in the normalized and tempered condition. Normalizing was carried out at a temperature of 1173K and tempering at 873K followed by cooling in air. The chemical composition of 3.5% nickel steel is given in Table - I.

The plates in as-received condition were cut and shaped to make experimental steel blocks of size 200mm x 70mm x 12mm. The edges of the blocks were grooved with single-vee shapes having included angle of 70°. The groove design is shown in Fig. 1a.

### Welding Parameters

All the joints for the present study were made by manual metal arc welding process with D.C. power source using two types of coated electrodes, namely Type - I (indigeneously available) and Type - II (imported). Before welding the coated electrodes were dried at a temperature of 573K for one hour and all the welding were made in flat position using identical welding parameters. (Table - II).

All completed welds were inspected by X-ray Radiographic Technique. The sound weld blocks were then sectioned into slices to make samples for mechanical, corrosion and microstructural studies.

Table - I

| | C | Si | Mn | Ni | S | P |
|---|---|---|---|---|---|---|
| Base Metal | 0.12 | 0.20 | 0.70 | 3.60 | 0.02 | 0.03 |

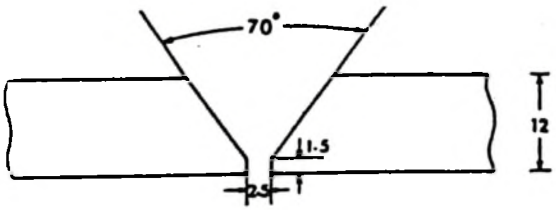


**Fig.1a :** Groove Design (Dimensions are in mm)

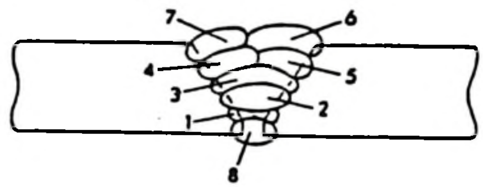


**Fig.1b :** Sequence of weld runs

## Mechanical Testing

Both transverse and all-weld tensile testing were carried out at room temperature (298K) in an Instron Universal Testing Machine of 10,000 Kg (10 ton) capacity and with a cross head speed of 3.3 x $10^{-5}$m/sec.

Charpy Impact Testing of the base and weld metals, prepared with two different electrodes, was carried out by Avery Charpy Impact machine at 172K. For weld joint, the V-notch was made perpendicular to the weld axis.

Microhardness Testing was carried out in Wolpert Testing Machine using 0.025Kg load and knoop indentor on polished and flat samples. Hardness measurement was taken at different positions across the weld metal (Fig.2).

Specimens for optical metallography were obtained from the transverse direction of the weld. (The quantitative assessment of the microstructure was made using a point counter. A minimum of 500 points were measured on each specimen). The microstructural constituents were identified according to the classification of IIW. [8]

**Table - II : Welding Parameters**

| Parameter | Value |
|---|---|
| Current (amp) | 110-130 |
| Voltage (Volts) | 32 |
| speed (m/sec) | 2.08 x $10^{-3}$ |
| Polarity | DC Electropositive |

## Environment sensitive failure tests

In order to assess stress corrosion cracking (SCC) propensities, tests were carried out in slow strain rate testing machine (SSRT) and corrosion fatigue (CF) tests at ambient

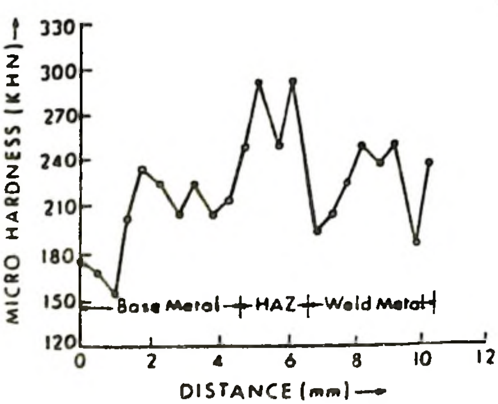


**Fig.2a :** Variation in Micro Hardness (KHN) across the weldment W1

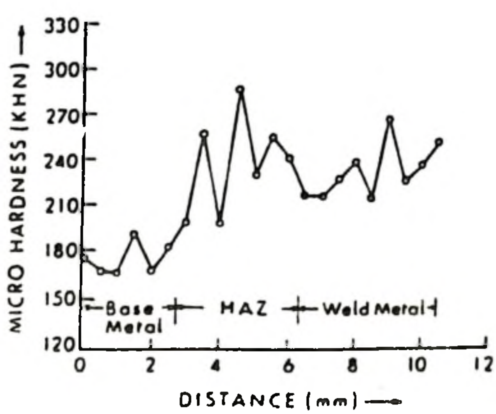


**Fig.2b :** Variation in Micro Hardness (KHN) across the weldment W2

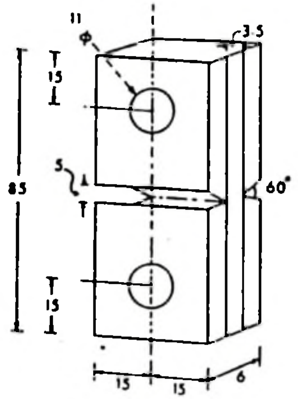


**Fig.3 :** S.E.N type grooved specimen for Environment Sensitive Failure Test (Dimensions are in mm)

and cryogenic temperatures at low cycle fatigue frequency of 0.2 Hz were carried out in specially designed fatigue machine. Single edge notch type test specimens (Fig. 3) were prepared from (i) the base and (ii) the weld metals (W1 & W2).

SSRT mode of testing was carried out at cross head speed (CHS) of $10^{-5}$mm. $s^{-1}$ (ferrous alloys testing at similar CHS, in sensitive environments, generates recordable environment sensitive failure effects on crack velocity and fracture appearance).

Low cycle fatigue (LCF) mode of testing at a frequency of 0.2 Hz (facilitates corrosion reaction time), at $\sigma$ max = 0.1 of the breaking load of the test specimen and at "R" value of 0.1, was carried out at ambient and 193K (±2K) temperatures for W2 material.

**Table - III Chemical Composition of Weld Metals with different Electrodes**

| | C | Si | Mn | Ni | S | P |
|---|---|---|---|---|---|---|
| Weld Metal (W1) (Type-I electrode) | 0.045 | 0.20 | 0.65 | 4.13 | 0.007 | 0.01 |
| Weld Metal (W2) (Type-II Electrode) | 0.038 | 0.266 | 0.47 | 3.93 | 0.0076 | 0.009 |

Cryogenic test cell for the LCF mode of testing was designed to contain specimen in test environment-methanol in a chamber surrounded by liquid nitrogen vapour chamber and vacuum chamber (vacuum in excess of $10^{-2}$ torr was maintained during test).

Crack extension was monitored (a) optically, using monocular telescope with vernier scale attachment and (b) by direct current potential drop (DCPD) technique adopted for these series of tests.

**Scanning electron microscopy (S.E.M.)** of charpy impact and corrosion test failure specimens was carried out to study fracture micromechanism.

## RESULTS AND DISCUSSION

### Characterisation of weld metal properties

The chemical composition of the weld metals is given in Table - III. There are small differences in the amount of C, Mn and Ni contents in the base and the two types of weld metals.

**Table - IV : Quantitative Metallographic Data of Weld Metal using different Electrodes**

| Material | Different Ferrite Morphologies (Vol %) | | |
|---|---|---|---|
| | G.B.F. | P.F. | A.F. |
| W1 | 26.2 | 17.60 | 56.6 |
| W2 | 28.4 | 20.46 | 51.4 |

A.F. = Acicular Ferrite G.B.F. = Grain Boundary Ferrite P.F. = Polygonal Ferrite

**Table - V**
**Transverse Tensile Testing Data of base metal (3.5% Nickel Steel) and Weld Metals using different Electrodes**

| Material | 0.2% Y.S. (MPa) | U.T.S. (MPa) | % Elongation | % Reduction In area | Remarks |
|---|---|---|---|---|---|
| Base Metal | 385 | 509 | 34 | 75 | |
| W1 | 391 | 519 | 28 | 72 | broke at base metal |
| W2 | 384 | 525 | 24 | 73 | broke at base metal |

**Fig.4 :** Microstructure of Base Metal (3.5% Ni steel) x 400

**Fig.5 :** Microstructure of Weld Metal (W2), x 400

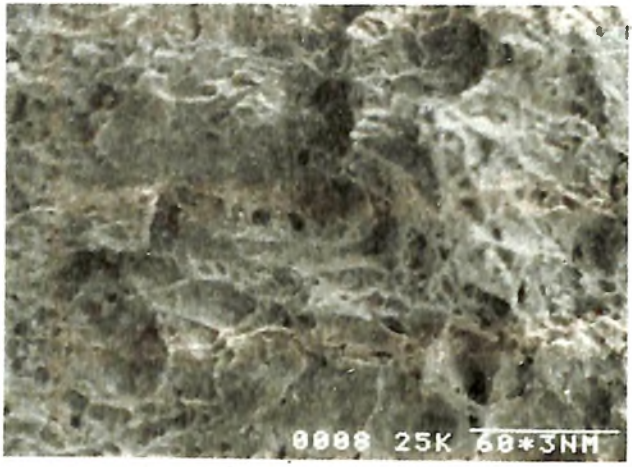


**Fig.6 :** S.E. fractograph of Charpy specimen of fractured (172K) Base Metal (3.5% Ni steel) x 500

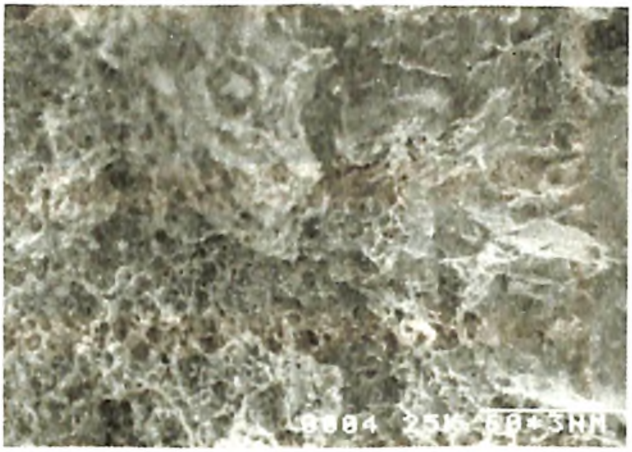

**Fig.7 :** S.E. fractograph of Charpy specimen of fractured (172K) Weld Metal (W2), x 500

The microstructure of the base metal consists of polygonal ferrite (light area) as shown in Fig. 4. Typical microstructure of the weld prepared by using Type-II electrode (W2) is presented in Fig. 5. The results of the quantitative assessment of the microstructure are given in Table - IV. This comparison shows that the welds consist of relatively high proportion of acicular ferrite with various amounts of grain boundary and polygonal ferrites.

Transverse and all-weld-metal tensile properties of different weld metals using two different types of electrodes are listed in Tables-V & VI respectively. All transverse tensile specimens broke at the base metals indicating strengthened weld metals compared to the base metal.

The charpy V-notch impact toughness values at 172K are shown in Table-VII. The better impact toughness at 172K associated with the weld metal (W1) produced by Type I electrode was probably due to higher amount of acicular ferrite (Table-IV) and inherently associated with lower strength of the weld metal (W1).

Table VI

All-Weld Tensile Testing Data of Weld metals using different Electrodes

| Material | 0.2% Y.S. (MPa) | U.T.S. (MPa) | % Elongation | % Reduction in area |
|---|---|---|---|---|
| W1 | 411 | 532 | 30 | 71 |
| W2 | 457 | 551 | 30 | 72 |

Table - VII

Charpy Impact Testing Values of Base Metals and Weld Metals using different electrodes at 172K

| Material | Charpy Impact Value at 172K (J) |
|---|---|
| Base Metal | 153.9 |
| W1 | 30.4 |
| W2 | 24.5 |

Table - VIII

Crack Velocity (C.V.) of Base Metal and Weld Metal Tested in SSRT mode at Laboratory Temperature (297K)

| Material | Environment | Average Crack Velocity (mm/sec) | | |
|---|---|---|---|---|
| | | Stage I | Stage II | Stage III |
| Base Metal | Air | # $(2 \times 10^{-6})$ | $(1 \times 10^{-6})$ | Tearing and |
| | Methanol | $6 \times 10^{-6}$ | $1.4 \times 10^{-4}$ | Yawning |
| W1 | Air | # $(7 \times 10^{-7})$ | $(7.5 \times 10^{-6})$ | Tearing and |
| | Methanol | $3 \times 10^{-6}$ | $2 \times 10^{-4}$ | Yawning |
| W2 | Methanol | $4.5 \times 10^{-6}$ | $6 \times 10^{-4}$ | Tearing and Yawning |

# Values given in bracket indicates coincidential approach to relate with environmental effect values.

Similar improvement of toughness with lowering of strength for similar microstructural constituents was previously reported [9].

The micromechanism of failure at 172K was studied by SEM. Evidently, failure (charpy) in the base metal was by transgranular cleavage (TGC) interspersed with discontinuous areas of micro void coalescence (MVC) mode. Qualitative assessment of fracture mode of weld metals produced by the different types of electrodes revealed, in general, crack propagation by TGC mode with discreet and varying amount of MVC. Fig. 6 represents the fracture mode of the base metal and Fig. 7 for W2.

### Environment sensitive failure tests

**a) SSRT in (i) Air and (ii) Methanol:** Data obtained from tests carried out in "slow strain rate testing" mode, at a CHS of $1 \times 10^{-5}$mm $s^{-1}$ in methanol environment at ambient laboratory temperature of 297K (approx) are related as in Fig. 8 and Table - VIII. Data obtained from these tests in methanol environment for the base and W2 material indicate effects of the test environments. Distinct differences were apparent when increasing load and increasing crack length with testing time were compared in the tests carried out in air and methanol environments in that - **i)** While tests in air monotonously increased stress and crack length in specimen with time till failure of the specimen had occurred, effect of methanol environment on the other hand, both on advancing crack length and increasing load with time, when related as shown schematically in Fig. 9, indicates crack progression in stages I, II & III till failure of the specimen had occurred. **ii)** Calculated crack advancement, i.e., crack velocity (CV), detailed in Table -VIII, indicates faster rate of crack growth in tests carried out in methanol environment. **iii)** Stage III crack progression in all specimens were discarded as discreet yawning of the crack was observed.

**Fracture Analysis :** In general fracture mode observed for tests in air was typically by microvoid coalescence (MVC) as in Fig. 10. Fracture appearance in specimen tested in methanol in the base and the weld metal (W2) are depicted in Figs 11 & 12. Initially, crack progression was by MVC at the notch root gave in to quasi brittle zone (Fig.11) outlined with flat ribbed facets indicates faster rate of crack growth in this region. Recorded crack growth data obtained from (base metal) the test indicates this area to have been generated effectively under environmental (methanol) influence.

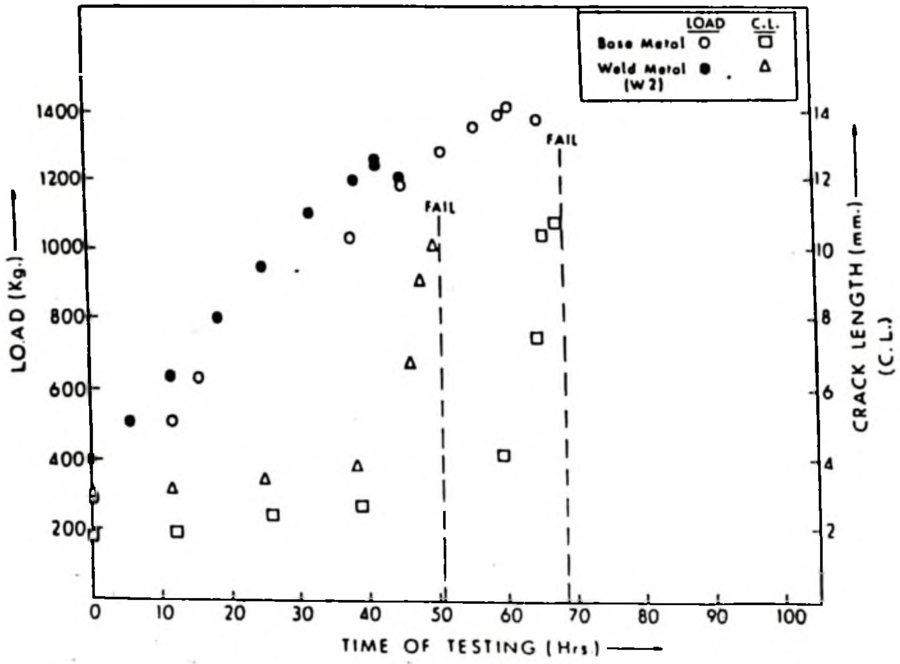


**Fig.8 :** Slow strain rate (C.H.S=$10^{-5}$ mm/sec) of base metal and weld metal (W2) tested in methanol.

**b) Low cycle fatigue (LCF) testing in (i) Air and (ii) Methanol**

Data obtained from selected tests are graphically presented in Fig. 13 and Table - IX.

Irrespective of the test metal composition, i.e., base metal or weld metal (W2), relative comparison of the recorded data highlights the following characteristics : **i)** In air-tests load-time relationship is a continuous slope to failure as expected, under constant displacement type fatigue loading [10, 11, 12]. **ii)** Crack growth rate (CV) in Air and MeOH remains similar in stage I. In stage II CV has effectively increased in methanol environment (Fig. 13). **iii)** Tests in acidified methanol did not significantly affect CV in the base metal vis-a-vis the weld metal tested in methanol. **iv)** Recorded low CVs in the gradually flattening out stage III region, for all test variation employed here in MeOH & MeOH + HCl environments indicate non-cracking conditions, as expected under constant displacement mode of fatigue testing [11,12].

**Fracture Analysis :** Fracture mode in air was by MVC. Environmental effects on fracture mode are shown in Figs 14(a) & (b) similar to those

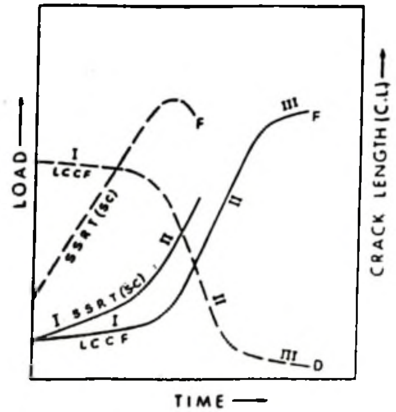


**LCCF** = Corrosion fatigue **SSRT** = Stress Corrosion **F** = Fail
**D** = Discontinue **I, II, III** = Stages of Development, load ---, CL.—.

**Fig.9 :** Load and crack progression in stages with time in SSRT and LCCF testing (schematic) modes.

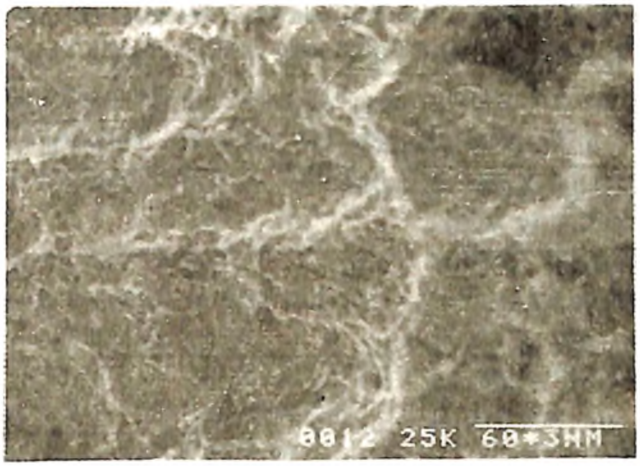


**Fig.10 :** S.E. fractograph of SSRT failed base metal (3.5% Ni steel) in air, x 500

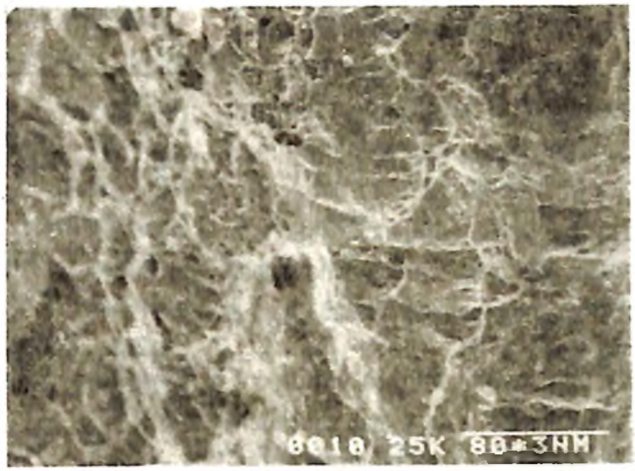


**Fig.11 :** S.E. fractograph of SSRT failed base metal (3.5% Ni steel) in methanol, x 380

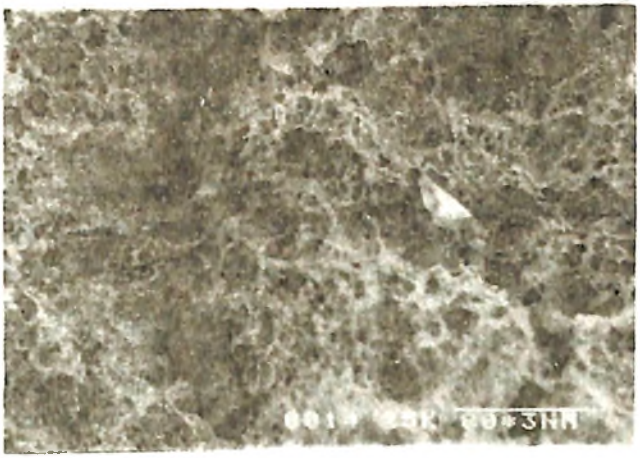

**Fig.12 :** S.E. fractograph of SSRT failed weld metal (W2) in methanol, x 380

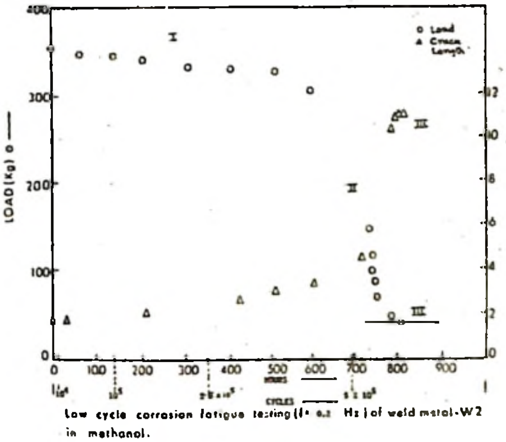


**Fig.13 :** Low cycle corrosion fatigue testing (f=0.2 Hz) of weld metal (W2) in methanol

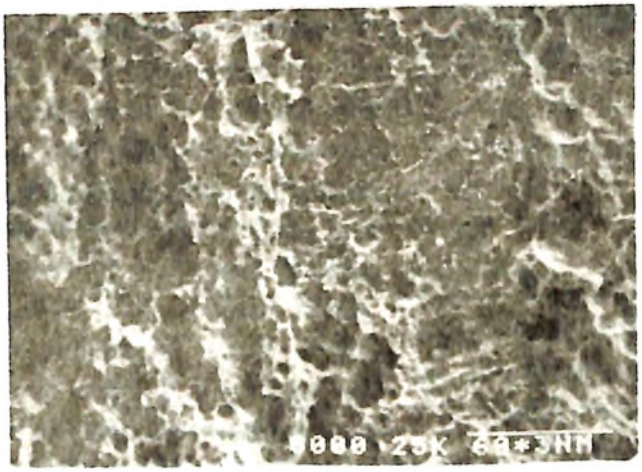

**Fig.14a :** S.E. fractograph of LCF failed weld metal (W2) in methanol at laboratory temperature, x 500


**Fig.14b :** S.E. fractograph of LCF failed weld metal (W2) in methanol at laboratory temperature, x 30 obtained in SSRT tests. Striations (Fig. 14b) observed are due to crack arrest markings as are generally observed in fatigue tests in air denoting mechanical aspiration. Corrosion fatigue effects are depicted in Fig. 14(a) including crack arrest phenomena separating quasi brittle continuous zones.

**(c) Low cycle fatigue mode of testing of weld metal specimen (W2) in methanol environment at cryogenic temperature** was carried out o characterize the effect of cryogenic temperature (e.g. at 193K) on the weld metal (W2) in a solvent environment.

**The Test :** LCF tests were carried out using SEN (Fig. 3) specimen contained in a specially designed test cell. Liquid nitrogen vapour was sparingly introduced in the cooling chamber to obtain the test temperature maintained at 193K (± 2K). Selected test temperature was 193K, close to the charpy test temperature at 172K which revealed brittle quasi-cleavage mode (>90% of the fractured surface).

**Table - IX**
**Crack Velocity (C.V.) of Base Metal and Weld Metal Tested in LCF at Laboratory Temperature (297K) and Cryogenic Temperature (193K)**

| Material | Environment | Average Crack Velocity (mm/sec) | | |
|---|---|---|---|---|
| | | Stage I | Stage II | Stage III |
| Base Metal | Methanol (294K) (+ 1% HCl) | $6 \times 10^{-7}$ | $1 \times 10^{-4}$ | $1 \times 10^{-6}$ |
| | Air (297K) # | ($2 \times 10^{-7}$) | ($4 \times 10^{-7}$) | $1 \times 10^{-6}$ (close to failure) |
| Weld Metal (W2) | Methanol (294K) | $4 \times 10^{-7}$ | $9 \times 10^{-5}$ | $3 \times 10^{-6}$ |
| | Methanol (193K) | | $1.2 \times 10^{-5}$ | |

# Values given in brackets indicates coincidental approach to relate with environmental effect values.

**Testing Load** ($\sigma_{max}$ and $\sigma_{min}$) **:** Introduction of liquid nitrogen vapour in the cooling chamber, surrounding the experimental chamber containing the test specimen immersed in the test environment-methanol, had decreased the test temperature (recorded - specimen surface temperature close to the notch) with concomitant increase in $\sigma_{max}$ (Fig 15), from the maintained $\sigma_{max}$ value at the ambient test temperature (297K) due to the constraint imposed by (i) the characteristic elastic/plastic domain change in the test material at cryogenic temperature and (ii) the constraint imposed by the constant displacement mode of fatigue loading (tension-tension) of the test specimen. Similarly, any increase in test temperature had decreased $\sigma_{max}$ along A-B as in Fig. 15. Changes in $\sigma_{min}$ with temperature was similar, effectively maintaining the consistency of the 'R' value at 193K. Tests in cryogenic temperature were continued at the achieved higher $\sigma_{max}$ and $\sigma_{min}$ values till failure had occurred progressively.

**Cryogenic Test Data :** Due to technical failure at the time of the experimental work DCPD system could not be engaged to monitor crack extension in the specimen. However, data obtained from the examination of fracture surface

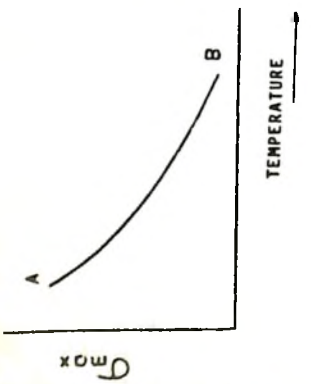


**Fig.15 :** Variation of Max. Load ($\sigma_{max}$) with Temperature

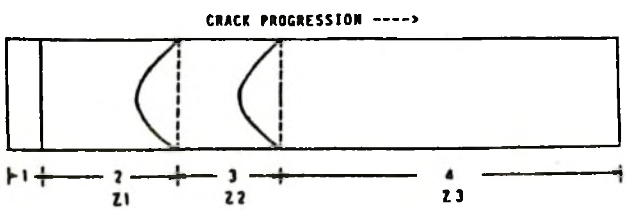


**Fig.17 :** Fracture Zone Profile as observed in S.E.M. examination of fracture surface obtained from cryogenic test and assessed by Scanning Microscopy

obtained from cryogenic test revealed separate zones developed under the prevailing test conditions were recorded and crack velocity was assessed (Fig.16). In the figure 16,

Area in1 $\rightarrow$ Notch

Area in 2 $\rightarrow$ Z1 - Precracked zone (5.0 mm)

Area in 3 $\rightarrow$ Z2 - Environment affected area generated by CF (2.61 mm)

Area in 4 $\rightarrow$ Z3 - Instant (Fast) fracture zone (7.92 mm).

[All measurements were carried out (i) using monocular microscope and counter checked by SEM].

**Fracture Analysis :** In scanning electron microscopic examination precracked zone (Z1 - generated by LCF) revealed quasi-ductile MVC mode typical of Q & T low alloy steel fracture under fatigue loading in air (Fig.10). This zone terminated at zone 2 (Z2). Z2 revealed quasi-cleavage facets interspersed with MVC. The fracture facets appeared (Fig. 17) blunt as would be expected under conjoint action of the test environment and cyclic loading sequences in the corrosion fatigue crack progression region. Areas covered under brittle facets increased along crack progression towards Z3, the fast fracture zone [the effect of cyclic (tension-tension) loading in methanol environment]. Z3 revealed quasi-cleavage, large cleaved zone with river line markings [Figs.17(b)&(c)]. Number of cleavaged facets increased with crack progression towards the terminal edges of the specimen. Fracture appearance in Z3 appeared similar to that observed in charpy specimen (W2) tested at 193K (± 2K) (Fig.18).

Consistent with the fracture zone profile, as in Fig. 16, it is assumed that the recorded total time to failure (57.5 hrs of the specimen) was required for the sub-critical crack to progress in environment sensitive failure dominated Z2 only. This zone is identified as due mainly to low temperature CF effect. Assessed crack velocity (CV) in this zone (Z2), $1.2 \times 10^{-5}$ mm $s^{-1}$ is a decade lower than the CV calculated for LCF in methanol at ambient test temperature found experimentally in this work.

Cracking potential at $K_Q$cf
i.e CF affected zone 2 can be related to :

$$K_{QCF} = \{[E/(1-\upsilon^2)][\gamma_p - ZF\rho\delta\eta/M]^{1/2}\}$$

Where

$E$ = Young's Modulus

$\upsilon$ = Poisson's Ratio

$\gamma_p$ = Plastic work necessary for crack progression (mechanical work)

$Z$ = Valency of the solvated ions.

$F$ = Faraday's constant.

$\rho$ = Density (of the alloy concerned)

$\delta$ = Approximate to COD on height of advancing crack front.

$M$ = Molecular mass of the metal

$\eta$ = Electro chemical potential

[13,14]

A reduction of the $\gamma_p$, plastic work term, will result from an increase in the effective yield stress due to lowering of temperature. This would mean an **incresed CV** in a CF environment if $\eta$ is unaffected. However, value of $\eta$ will decrease with lowering of temperature or decreasing time required for $\eta$ potential to be effective [10]. In this work lowering of test temperature by 100K (to 193K) has increased elastic stress level by :

(E X Th. coef.) X Temp. difference
where

*E = young's modulus*
*Th. coef. = Thermal Coeffeicient*
*(E & Th. coef. is in Giga Pascal)*

= [(2 x 10'') (2 x $10^{-3}$] 100
= 400 Mpa (approx.)

i.e. increased stresses viz. room temperature would be available for plastic work at 193K.

This increment in stress level at 193K is expected to increase CV in Zone 2. However, in balance effect of lowering the temperature decreased corrosion potential $\eta$ by

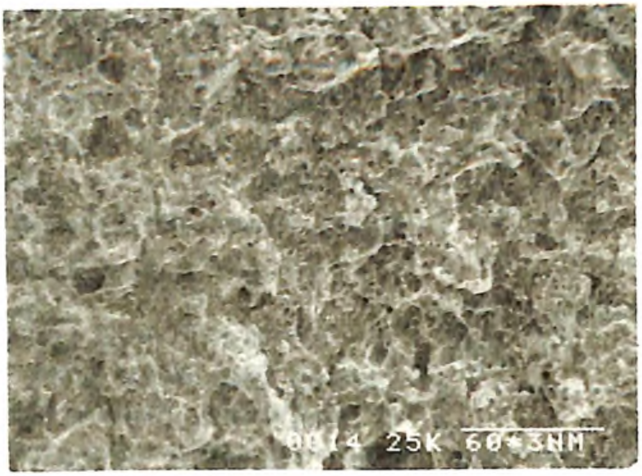


**Fig.17a :** S.E. fractograph of LCF failed weld metal (W2) in methanol at 193K at — Z2, x 500

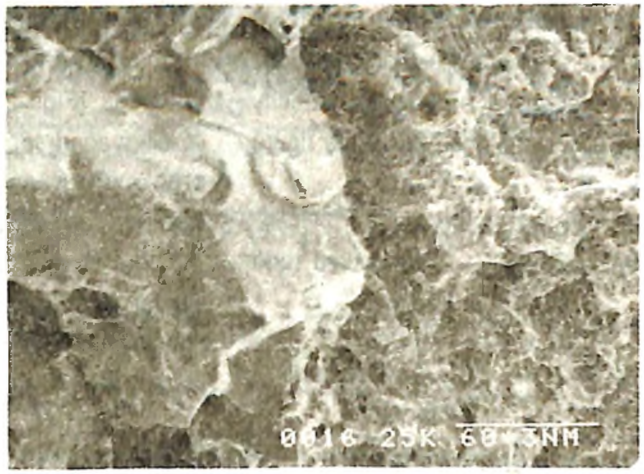


**Fig.17b :** S.E. fractograph of LCF failed weld metal (W2) in methanol at 193K at — Z2-Z3, x 500


**Fig.17c :** S.E. fractograph of LCF failed weld metal (W2) in methanol at 193K at — Z3, x 1K


**Fig.18 :** S.E. fractograph of charpy specimen (W2) fractured at 193K, x 1K

a margin which has decreased corrosion fatigue crack velocity (at 193K) compared with CV at room temperature where $\gamma_p$ term is dominant.

In zone 3 (Z3) crack progression was instantaneous - as in quasi-cleavage brittle failure (known to be at the speed of sound) [14]. The dominating fracture mode observed in this zone is large cleavage facets occasionally terminating at grain boundaries (Fig. 17c). Transgranular crack progression was also evident (Fig. 17b). Crack arrest markings evident in Z2 (Fig. 17b), for instance, were not observed in Z3 (Fig. 17c) at comparable resolution (SEM), which also indicates subcritical crack growth under corrosion fatigue conditions as in Z2 of W2 material was not present in zone 3.

## CONCLUSION

The following conclusion with regards to the characterisation of specific properties of the tested weld metals can be drawn : **i)** In general, all weld metals exhibit poor charpy impact toughness at 172K. **ii)** Scanning electron microfractographs revealed, in general, crack progression by transgranular cleavage mode with discreet and varying amount of micro void coalescence. Prevalence of secondary cracking in fracture surfaces obtained from weld metals and the amount of transgranular quasi cleavage type fracture mode indicates greater brittle failure propensities compared with MVC dominated fracture surface obtained from base metal tested under similar test conditions.

From the series of environment sensitive failure tests (stress corrosion and low cycle corrosion fatigue tests), limited in some respects, following areas, as concluding remarks, have emerged :

In all three modes of testing, namely (i) SSRT, (ii) LCF and (iii) cryogenic (LCF), effects due to the test environment-methanol, a solvent, were apparent in that -

a) Crack progression in methanol environment was faster by more than a decade vis-a-vis the CV recorded for tests in air,

b) In SSRT & LCF testing in methanol environment and at the test parameters used in this experimental work stress corrosion and corrosion fatigue effects were identified in stage II zone where CV was at maximum. Examination of fracture surface in this zone revealed quasi-brittle fracture mode, secondary cracks, crack arrest markings and corrosion effect blunting the fracture facets are typical of fracture modes revealed in SC & CF dominated failure of ferrous material, in general,

c) In LCF modes of testing brittle to ductile transition at critical load/stress, similar to $K_{QCF}$, was identified, a parameter indicating safe loading condition in specific environmental use,

d) In these cryogenic tests, the effect of methanol environment at cryogenic temperature (193K) revealed CF cracking propensities and observed catastropic failure also indicated unpredictable life performance of these welded material in cryogenic use,

e) Crack progression in SC and CF continuum, in weld metal, as shown in this work demand critical examination to avoid such occurrences. Solvent such as methanol, under critical loading, monotonous and cyclic, as used in this experimental work, could initiate environment sensitive brittle failure in weld metal continuum in 3½% Ni steel.

In order to avoid unpredictable failure in these material environment systems it would be prudent to ensure uses :

i) When under monotonous loading conditions (e.g. static reserve tank), at ambient temperatures, at strains on the welded section pertaining to Stage I (steady state sub-critical crack growth), enables greater predictability to failure,

ii) and when under cyclic loading conditions (e.g. during transportation, continuous loading and unloading) at temperatures higher than 193K (predictably, decrease amount of brittle fracture mode), at strains pertaining either to Stage I (steady sub-critical crack growth) or Stage III ($K_{QCF}$ - no cracking at ambient temperatures) and at loading frequencies higher than 0.17 Hz would decrease material-environment electrochemical/ chemical reaction time improving life performance.

**ACKNOWLEDGEMENTS**

Authors are thankful to D.S.T. to provide financial support and M/s ESAB India Ltd., Khardah, 24-Parganas (N), W.B. for their kind co-operation in assisting with testing facilities.

**REFERENCES**

1. Wormington H., A Problem in Welding 3.5% Nickel Steel Welding and Metal Fabrication, Vol.35(6), 1967, p. 253-358

2. Ishimaru Y., Kobayashi H., Okada T. and Tomiyasu F., Automatic Welding of 3.5% Nickel Steel, Welding J., Vol. 57(9), 1978, p. 273-280.

3. Thorneycroft D. R., Jordan D.E. and Crane L. W., 'Some Metallurgical Observations on 3.5% Nickel Steel Weld Metal with respect to properties . at Sub-Zero Temperature', Brit, Welding, J., Vol. 19(5), 1963, P. 212-221.

4. Dawas M. G. and Saunders G. G., Influence of Heat Treatment and Thickness on Brittle Fracture in 3.5% Ni Steel Weldments, Metal Constr., Vol. 5(3), 1973, p. 94-101.

5. Watanabe Masaki, 'Progress of Chemical Plant and Material/ Welding Technology in Japan', IIW Doc. No. XI-446-86.

6. Farrar R. A. and Harrison P. L., 'Acicular Ferrite in Carbon-Manganese Weld Metals : an overview', Journal of Materials Science, Vol. 22, 1982, p. 3812-3820.

7. Tweed J. H. and Knot J. F., 'Effect of reheating on Micro-sturucture and Toughness of C-Mn Weld Metal', Metal Science, vol. 17(2), 1983, p. 45-54.

8. Dunkan A., 'Guide to the Examination of Ferrite Steel Weld Metals', IIW-Doc. No. IXJ-123-87.

9. Dolby R.A., "Factors controlling weld toughness — The present position, Part 2 : Weld metals", Research Report 14/1976/M, The Welding Institute, Abington, May, 1976

10. Majumdar. P., "Characteristic effects of LCF testing by constant displacement mode", 'Proceedings of First Mexican Symposium on Metallic Corrosion, Ed : Maldonado, L & Casul, p., (March, 1994) Mexico.

11. Majumdar P. and Scully J. C., Corr. Sci., 19, 1979, 141.

12. Parkins R. N., ASTM-STP/665, 1974.

13. Burke J. J. and Weiss V., Ed., Fatigue : Environment and Temperature Effects, Sagamore Army Mater. Res. Conf. Proc., Vol. 27, 1983.

14. Parkins R. N. et al "Crack growth mechanism", Proceedings of Int. Conf; Met. Soc. (U.K.) guildford (1977), Ed, Swan, Ford, Westwood.

☒